

Diagnostic Function of 3-Tesla Magnetic Resonance Imaging for the Assessment of Brachial Plexus Injury

Annals of Neurosciences
27(3-4) 124–130, 2020
© The Author(s) 2021
Reprints and permissions:
in.sagepub.com/journals-permissions-india
DOI: 10.1177/0972753120963299
journals.sagepub.com/home/aon



Nguyen Duy Hung^{1,2}, Nguyen Minh Duc^{3,4} , Nguyen Thi Xoan¹, Ngo Van Doan⁵,
Tran Thi Thanh Huyen⁶, and Le Thanh Dung²

Abstract

Background: This study aimed to evaluate the diagnostic function of 3-Tesla (T) magnetic resonance imaging (MRI) during the assessment of brachial plexus injury (BPI), in comparison with intraoperative findings.

Methods: A retrospective study was performed on 60 patients (47 men and 13 women), who had clinical manifestations of BPI, underwent 3T MRI of the brachial plexus, and were surgically treated at the Viet Duc and Vinmec Times City hospitals, in Hanoi, Vietnam, from March 2016 to December 2019. Preganglionic and postganglionic lesion features were identified on MRI. The diagnostic function of MRI features for the determination of BPI was evaluated and correlated with intraoperative findings.

Results: The root avulsion and pseudomeningocele preganglionic injuries were observed in 57% and 43% of MRIs, respectively, and were commonly observed at the C7 and C8 roots. Nerve disruption and nerve edema were observed in 47.56% and 33.53% of MRIs, respectively, and were commonly observed at the C5 and C6 roots. The sensitivity, specificity, accuracy, positive prognostic value, and negative prognostic value of 3T MRI were 64.12%, 92.90%, 80.33%, 87.50%, and 76.96%, respectively, for the diagnosis of total avulsion, and 68.52%, 83.33%, 80.67%, 47.44%, and 92.34%, respectively, for the diagnosis of nerve disruption.

Conclusion: MRI offers valuable details regarding the location, morphology, and severity of both preganglionic and postganglionic injuries during the preoperative diagnosis of BPI. However, this modality played a moderate diagnostic role. Therefore, 3T MRI should be used as a supplemental evaluation, coupled with clinical tests and electromyography, to determine the most appropriate treatment strategies for BPI patients.

Keywords

Brachial plexus injury, preganglionic lesions, postganglionic lesions, MRI, diagnostic function

Abbreviations

ACC: Accuracy
BPI: Brachial plexus injury
CISS: Coronal constructive interference steady-state
MRI: Magnetic resonance imaging
NPV: Negative predictive value
PACS: Picture archiving and communication system
PPV: Positive predictive value
Se: Sensitivity
Sp: Specificity
STIR: Short-tau inversion recovery
2D: 2-dimension
3D: 3-dimension

and sensation, which deteriorate the quality of life for patients.¹ BPI often occurs in young people, primarily due to traffic accidents. The treatment and prognosis of BPI rely on the site and severity of the injury, as well as the interval between the accident and surgery. BPI can be classified into preganglionic and postganglionic

¹ Department of Radiology, Hanoi Medical University, Hanoi, Vietnam

² Department of Radiology, Viet Duc Hospital, Hanoi, Vietnam

³ Department of Radiology, Pham Ngoc Thach University of Medicine, Ho Chi Minh City, Vietnam

⁴ Department of Radiology, Children's Hospital 2, Ho Chi Minh City, Vietnam

⁵ Department of Radiology, Vinmec Times City Hospital, Hanoi, Vietnam

⁶ Department of Maxillofacial Plastic and Aesthetic Surgery, Viet Duc Hospital, Hanoi, Vietnam

Introduction

Brachial plexus injury (BPI) accounts for 1% of all major injuries and can adversely affect upper-limb motor functions

Corresponding author:

Nguyen Minh Duc, Department of Radiology, Pham Ngoc Thach University of Medicine, Ho Chi Minh City, Vietnam.
E-mail: bsnguyenminhduc@pnt.edu.vn



lesions, and each type of lesion is associated with distinct surgical procedures.² The precise diagnosis of the lesion is, therefore, necessary to develop an effective treatment plan that can improve neurological symptom recovery.³ BPI diagnosis is often based on clinical examinations, imaging tests, and electromyography. However, clinical tests and electromyography have limited the ability to determine the site or extent of early-stage injury.⁴ Magnetic resonance imaging (MRI) for the brachial plexus is a noninvasive and nonradiative method for the assessment of preganglionic and postganglionic lesions. Past findings have shown that MRI contains more details than ultrasound, electromyography, or intraoperative somatosensory-evoked potentials for the evaluation of BPI.^{5,6} The 3-Tesla (T) MRI systems provide a higher signal-to-noise ratio and spatial resolution than low-magnetic field MRI systems, providing improved 2- and 3-dimensional (2D and 3D, respectively) image quality for BPI assessments, particularly for postganglionic lesions.^{4,7}

Several studies have investigated the value of MRI during the diagnosis of BPI, without comparing against gold-standard diagnostic modalities, such as surgery.^{8,9} Other reports have contrasted the MRI results with those found during operations, but most of these studies have been based on low-magnetic-field MRI devices.^{10–12} The goal of this study was to evaluate the diagnostic function of 3T MRI for BPI in comparison with intraoperative findings.

Materials and Methods

Study Population

A retrospective study was performed on 60 patients (47 men and 13 women, aged 0–56 years, with a median age of 20.28 years), who had clinical manifestations of BPI, underwent 3T MRI of the brachial plexus, and were treated by nerve surgery at the Viet Duc and Vinmec Times City hospitals, in Hanoi, Vietnam, from March 2016 to December 2019. The imaging and surgical protocols were uniform at both centers. This retrospective study was approved by institutional review board (Ref: 6811/QĐ-ĐHYHN dated 16 December 2019), and the informed consent of patients was waived.

MRI Technique

The MRI examinations were conducted on either a Siemens 3T MAGNATOM Skyra (Siemens Medical Systems, Erlangen, Germany) or 3T GE SIGNA Pioneer (GE Healthcare, Milwaukee, USA) with a head and neck joint coil and body coil, covering the neck and shoulders in adults, and a flex large coil, for children. Patients were scanned supine in a craniocaudal direction. Padding and cushions were placed under the patient's shoulders and head to reduce the curvature of the cervical spine. The demands of declining swallow and movement were made during the MRI procedure.

The scanning field was limited, from the superior border of the C3 level to the inferior border of the T3 level and from the anterior border of the spinal bodies to the posterior border of the spinal canal. The bilateral armpits were also involved. The scanning protocol included the following sequences: (1) sagittal T2-weighted image (T2WI), (2) coronal T1-weighted image (T1WI), (3) coronal short-tau inversion recovery (STIR), (4) coronal constructive interference steady-state (CISS), and (5) axial CISS sequences. No contrast agent was administered in any case.

Images were transferred to a picture archiving and communication system (PACS) workstation (Carestream PACS; Carestream Health, Eemnes, Netherlands), and the maximum intensity projection (MIP) and multiplanar reconstruction were used to assess lesions on the STIR and CISS sequences. Images were analyzed by single observer who had 10-year MRI experience in neuroradiological field along with national medical practicing certificate.

Image Analysis

BPI diagnoses were classified into preganglionic and postganglionic lesions, depending on the location of the dorsal ganglia.^{13,14} The indirect features of preganglionic lesions included the following: spinal cord offset, defined as the displacement of the spinal cord to either the injured side or the contralateral side⁴; spinal cord edema, defined as a focal hyperintense and enlarged region on T2WI, in the acute phase; and intramedullary hemorrhage, defined as a focal hyperintense area, surrounded by a hypointense rim that reflected hemosiderin deposition on T2WIs.^{14,15}

The direct features of preganglionic lesions included the following: rootlet avulsion (Figure 1), defined as a disruption between the rootlets and the cord,¹⁴ for which total avulsion was defined as the disruption between all anterior and all posterior rootlets and the cord, whereas partial avulsion was defined as the disruption between all anterior, all posterior, or some anterior and posterior rootlets and the cord¹⁶; and pseudomeningocele, defined as the leakage of cerebrospinal fluid that extended beyond the spinal foramina into the adjacent tissues.^{2,4,14,17}

The features of postganglionic lesions included the following: nerve disruption (Figure 2), defined as nerve discontinuity, with distal retraction^{14,18}; nerve edema, defined as a continuous nerve with diffuse hyperintense regions and enlargement on T2WI or STIR^{14,18}; and neuroma formation, defined as a focal nerve enlargement, which appears hyperintense on T2WI or STIR.^{13,14}

Statistical Analysis

SPSS version 22 was for data analysis (IBM Corp., New York, USA). Quantitative variables are displayed as medians. Categorical variables are displayed as numbers and percentages. The diagnostic function of MRI for BPI in

comparison with final surgical results was determined based on the sensitivity (Se), specificity (Sp), accuracy (ACC), negative predictive value (NPV), and positive predictive value (PPV). Chi-squared or Fisher’s exact test was used to compare the differences between MRI and intraoperative findings, if appropriate. A significance level of $p < 0.05$ was employed.

Results

In this study, the most common cause of BPI was traffic accidents (73.3%), followed by trauma during childbirth (23.3%). Closed and open injuries accounted for 96.7% and 3.3% of BPI cases, respectively. Additionally, 45% of cases presented associated injuries. The median interval between injury and MRI scan was 53 days (range, 17–419), with 15% of cases scanned within 30 days of injury and 58.3% of cases scanned between 30 and 90 days after injury. The median interval between injury and surgical intervention was 98 days, with 85% of cases being operated on within 180 days of the injury.

Basic MRI Features of BPI

Among the observed indirect preganglionic lesions, spinal cord offset and intramedullary hemorrhage were noticed in 5 cases and 1 case, respectively. No spinal cord edema was observed.

The observed preganglionic lesion features are shown in Table 1. Root avulsion and pseudomeningocele rates were 57% and 43%, respectively, and were commonly observed at the C7 and C8 roots. Rootlet avulsion, without pseudomeningocele, was observed in 14% of cases.

The observed postganglionic lesion features are shown in Table 2. Nerve disruption and nerve edema rates were 47.56%

and 33.53%, respectively, and were commonly observed at the C5 and C6 roots.

Table 1. The Features of Preganglionic Lesions

	C5 Root n (%)	C6 Root n (%)	C7 Root n (%)	C8 Root n (%)	T1 Root n (%)	Total n (%)
Total avulsion	6 3	13 6.50	29 14.50	29 14.50	19 9.50	96 48
Partial avulsion	3 1.50	5 2.50	6 3	3 1.50	1 0.50	18 9
Pseudomeningocele	3 1.50	11 5.50	26 13	27 13.50	19 9.50	86 43
Total	12 6	29 14.50	61 30.50	59 29.50	39 19.50	200 100

Table 2. The Features of Postganglionic Lesions

	C5 Root n (%)	C6 Root n (%)	C7 Root n (%)	C8 Root n (%)	T1 Root n (%)	Total n (%)
Nerve disruption	28 17.07	23 14.02	13 7.93	6 3.66	8 4.88	78 47.56
Nerve edema	13 7.93	12 7.31	8 4.88	10 6.10	12 7.31	55 33.53
Neuroma formation	8 4.88	9 5.49	6 3.66	5 3.05	3 1.83	31 18.91
Total	49 29.88	44 26.82	27 16.47	21 12.81	23 14.02	164 100

Table 3. Diagnostic Function of MRI for the Detection of Nerve Root Avulsions

Total Avulsion Confirmed by MRI		Total Avulsion Confirmed by Surgery		Se (%)	Sp (%)	ACC (%)	PPV (%)	NPV (%)	P-Value
		Yes	No						
C5 root	Yes	6	0	31.58	100	78.33	100	75.93	<0.001
	No	13	41						
C6 root	Yes	12	1	46.15	97.06	75	92.31	70.21	<0.001
	No	14	33						
C7 root	Yes	25	4	78.13	85.71	81.67	86.21	77.42	<0.001
	No	7	24						
C8 root	Yes	24	5	85.71	84.38	85	82.76	87.10	<0.001
	No	4	27						
T1 root	Yes	17	2	65.38	94.12	81.67	89.47	78.05	<0.001
	No	9	32						
Total	Yes	84	12	64.12	92.90	80.33	87.50	76.96	<0.001
	No	47	157						

Abbreviations: ACC = accuracy, NPV = negative predictive value, PPV = positive predictive value, Se = sensitivity, Sp = specificity.

Table 4. Diagnostic Function of MRI for the Detection of Nerve Disruptions

Disruption Confirmed by MRI	Disruption Confirmed by Surgery		Se (%)	Sp (%)	ACC (%)	PPV (%)	NPV (%)	P-Value	
	Yes	No							
C5 root	Yes	16	12	69.57	67.57	68.33	57.14	78.13	0.005
	No	7	25						
C6 root	Yes	11	12	68.75	72.73	71.67	47.83	86.49	0.003
	No	5	32						
C7 root	Yes	4	9	66.67	83.33	81.67	30.77	95.74	0.005
	No	2	45						
C8 root	Yes	3	3	60	94.54	91.67	50	96.30	<0.001
	No	2	52						
T1 root	Yes	3	5	75	91.07	90	37.5	98.08	<0.001
	No	1	51						
Total	Yes	37	41	68.52	83.33	80.67	47.44	92.34	<0.001
	No	17	205						

Abbreviations: ACC = accuracy, NPV = negative predictive value, PPV = positive predictive value, Se = sensitivity, Sp = specificity.

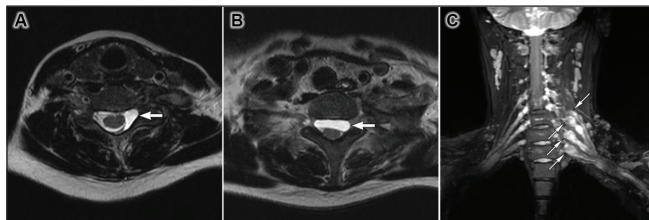


Figure 1. Rootlet avulsion of the left brachial plexus in a 35-year-old female with 3-month history of motorbike accident. Axial CISS (A) shows a pseudomeningocele (white arrow) located laterally to the spinal cord at the level of left C5-C6 foramen with no attachment of the left roots to spinal cord. Axial CISS (B) shows a pseudomeningocele (white arrow) located anteriorly to spinal cord at the level of C6-C7 foramen with the posterior displacement of the spinal cord. Coronal STIR with MIP reconstructed (C) shows the distal end retraction of left C5, C6, C7, and C8 nerve roots (white arrows). CISS, coronal constructive interference steady-state; MIP, maximum intensity projection; STIR, short-tau inversion recovery.

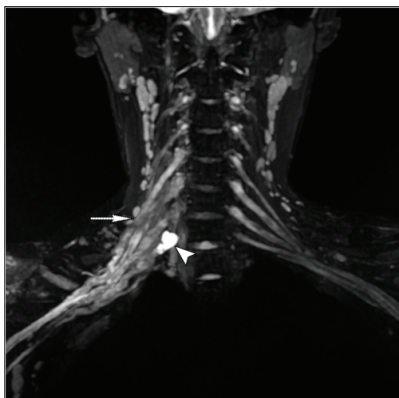


Figure 2. Nerve disruption in a 28-year-old male with 2-month history of motorbike accident. Coronal STIR with MIP reconstructed image shows the disruption of the right C5 nerve root (white arrow) with minimal retraction, the pseudomeningocele of the right C8 nerve root (arrowhead). MIP, maximum intensity projection; STIR, short-tau inversion recovery.

Diagnostic Function of MRI for BPI

MRI provided Se, Sp, ACC, PPV, and NPV values of 64.12%, 92.90%, 80.33%, 87.50%, and 76.96%, respectively, for the diagnosis of total avulsion, and the Se values for the detection of total avulsion at the C7, C8, and T1 roots were higher than those at the C5 and C6 roots (Table 3).

MRI provided Se, Sp, ACC, PPV, and NPV values of 68.52%, 83.33%, 80.67%, 47.44%, and 92.34%, respectively, for the diagnosis of nerve disruptions, and the Se and Sp values for the detection of nerve disruption at the C8 and T1 roots were higher than those at the C5, C6, and C7 roots (Table 4).

Discussion

The interval between an accident and treatment plays a major role in the rehabilitation of neurological symptoms. Open injuries are also recognized to require expeditious surgery.¹⁹ In addition, in case of closed injuries with root avulsions or nerve damage, surgery should be considered within 3 weeks.²⁰ When nerve edema is presented with associated injuries, treatment of associated injuries should be prioritized, with clinical follow-up for nerve edema. Unless the clinical signs indicate sluggish to no improvement, surgery can generally occur within 6 months, to prevent nerve degeneration.¹⁹⁻²² Our results showed that the bulk of surgical operations were conducted within 3 months of damage, with a median accident-to-surgery interval of 93 days. Previous studies have seldom reported the timing of MRI scans. O'Shea et al. stated that MRI scans should be performed after a minimum of 3 weeks because pseudomeningocele can be misdiagnosed due to the attachment of blood clots in the spinal canal to breaches

of the dura.⁶ Several reports have suggested performing MRIs within 3 months to diagnose traumas related to birth and delivery.^{23,24} In the present study, the median interval between injury and MRI scan was 53 days, due to 45% of cases having associated injuries.

Many previous studies have identified preganglionic lesion features on MRI scans.^{2,11,13,25-29} Spinal cord abnormalities are the suggestive findings of root avulsion.^{11,27} According to Hems et al.¹¹, root avulsions were often observed at the C7 and C8 roots. Wade et al. reported that the detection rates for root avulsion and pseudomeningocele were 60% and 40%, respectively, and primarily occurred at the C7 and C8 roots.² Zhang et al.¹³ reported rates of 42.5% and 12.5%, respectively, whereas Acharya et al.²⁹ reported rates of 56.3% and 43.8%, respectively. Our study showed similar results, with a detection rate for root avulsion of 57%, and the C7 and C8 roots were the common sites of root avulsion and pseudomeningocele. The elevated rates of root avulsions detected at the C7 and C8 roots are likely due to the absence of ligaments for these roots in the spinal foramina.^{29,30} Partial avulsion was rarely detected at the T1 root, and the detection rate for this lesion in our study was comparable to that reported by Carvalho et al.¹⁰ Some authors have suggested that pseudomeningocele is an unreliable finding for the diagnosis of root avulsion.^{2,14,15} According to Van et al., 15% of pseudomeningocele incidents were detected without root avulsion, and conversely, 20% of root avulsion incidents were observed without pseudomeningocele.¹⁵ Our findings agree with previous reports. Postganglionic lesions have been described in several previous studies.^{3,4,13,29} The rates of nerve disruption and nerve edema reported by Zhang et al. were 34.8% and 47.8%, respectively, which were similar to the rates of detection in our study. Zhang et al. also found that the C8 root was the most vulnerable site, whereas our study found that the C5 and C6 roots were the most vulnerable.¹³ This inconsistency may be due to discrepancies in the sample sizes and injury mechanisms.

A systematic review by Wade et al. showed that MRI could detect nerve root avulsions with Se values that ranged from 77% to 98%, with Sp values that ranged from 42% to 90%.²⁸ Another study by Wade et al. found that the Se, Sp, ACC, PPV, and NPV values were 68%, 85%, 79%, 75%, 81%, respectively, for the detection of root avulsion and 40%, 87%, 68.3%, 65%, 69%, respectively, for the detection of pseudomeningocele, using a 1.5 T MRI.² In a BPI study using a 3T MRI, Zhang et al.¹³ reported Se, Sp, and ACC values of 93.55%, 71.43%, and 89.4%, respectively, for the identification of preganglionic lesions. A study performed by Acharya et al. showed that MRI detection resulted in Se, Sp, ACC, PPV, and NPV values of 39%, 75%, 51%, 75%, and 39%, respectively, for the diagnosis of BPI in adults, with low sensitivity at the C5 and C6 roots.²⁹ Our study evaluated BPI in both children and adults, showing that 3T MRI could diagnose total avulsion with Se, Sp, ACC, PPV, and NPV

values of 64.12%, 92.90%, 80.33%, 87.50%, and 76.96%, respectively. The Se for the evaluation of root avulsion at the C5 and C6 levels was low in our study (31.58% and 46.15%, respectively), similar to those in the study by Acharya et al.²⁹ This result may be due to the limited subarachnoid space at levels C5 and C6, and the angle of the rootlets may influence the image quality.¹⁰ The detection of postganglionic lesions on MRI scans was mentioned in several studies.^{13,29} Zhang et al. revealed that MRI diagnosed nerve disruption with Se, Sp, and ACC values of 91.3%, 60%, and 85.71%, respectively. The Se value reported by Zhang et al. may be greater than our result possibly because the diffusion-weighted imaging used by Zhang et al. resulted in better image quality for the dorsal ganglia and the nerve root.¹³ The study by Acharya et al. resulted in Se and Sp values of 87% and 26%, respectively, for the detection of trunk and cord lesions.²⁹ The author suggested that the low Sp value was due to the overestimation of hyperintense lesions in the trunk and cord. Therefore, our findings are in agreement with previous studies.

Our study has some drawbacks. First, our study analyzed a small sample size from only two imaging centers, which may reduce the representative value of this study. Second, long scanning times can result in movement artifacts, particularly in traumatic patients, which can negatively impact image quality. In addition, in this study the time between the injury and MRI scanning was various among patients which would lead to an uncontrolled bias. A tabulation of the same in all patients would be more worthwhile in further investigations. Future studies should be performed on larger sample sizes, with shorter scanning times and same delay between the injury and MRI scanning, to validate and compare against our current results.

Conclusion

Our results showed that 3T MRI can provide valuable information regarding the location, morphology, and extent of both preganglionic and postganglionic lesions during the preoperative diagnosis of BPI. However, the sensitivity of this modality was modest. Thus, 3T MRI may be used as an additional examination, in combination with clinical tests and electromyography, to determine the most appropriate therapeutic strategies for patients.

Authors' Contribution

NDH and NMD contributed equally to this article as first authorship. NDH and NMD gave a substantial contribution in acquisition, analysis, and data interpretation. NDH and NMD prepared, drafted, and revised manuscript critically for important intellectual content. Each author gave the final approval of the version to be published and agreed to be accountable for all aspects of the work, ensuring that questions related to the accuracy or integrity of any part of the work are appropriately investigated and resolved.

Declaration of Conflicting Interests

The authors declared no potential conflicts of interest with respect to the research, authorship and/or publication of this article.

Ethical Statement

This retrospective study was approved by institutional review board (Ref: 6811/QĐ-ĐHYHN dated 16 December 2019) and the informed consent of patients was waived.

Funding

The authors received no financial support for the research, authorship, and/or publication of this article.

ORCID iD

Nguyen Minh Duc  <https://orcid.org/0000-0001-5411-1492>

References

- Midha R. Epidemiology of brachial plexus injuries in a multitrauma population. *Neurosurgery* 1997; 40(6): 1182–1189.
- Wade RG, Itte V, Rankine JJ, et al. The diagnostic accuracy of 1.5T magnetic resonance imaging for detecting root avulsions in traumatic adult brachial plexus injuries. *J Hand Surg Eur* 2018; 43(3): 250–258.
- Yang J, Qin B, Fu G, et al. Modified pathological classification of brachial plexus root injury and its MR imaging characteristics. *J Reconstr Microsurg* 2013; 30(3): 171–178.
- Qin BG, Yang JT, Yang Y, et al. Diagnostic value and surgical implications of the 3D DW-SSFP MRI on the management of patients with brachial plexus injuries. *Sci Rep* 2016; 6(1): 35999.
- Lapegue F, Faruch-Bilfeld M, Demondion X, et al. Ultrasonography of the brachial plexus, normal appearance and practical applications. *Diagn Interv Imaging* 2014; 95(3): 259–275.
- O’Shea K, Feinberg JH, and Wolfe SW. Imaging and electrodiagnostic work-up of acute adult brachial plexus injuries. *J Hand Surg Eur* 2011; 36(9): 747–759.
- Chhabra A, Thawait GK, Soldatos T, et al. High-resolution 3T MR neurography of the brachial plexus and its branches, with emphasis on 3D imaging. *AJNR Am J Neuroradiol* 2013; 34(3): 486–497.
- Takahara T, Hendrikse J, Yamashita T, et al. Diffusion-weighted MR neurography of the brachial plexus: Feasibility study. *Radiology* 2008; 249(2): 653–660.
- Qiu TM, Chen L, Mao Y, et al. Sensorimotor cortical changes assessed with resting-state fMRI following total brachial plexus root avulsion. *J Neurol Neurosurg Psychiatry* 2014; 85(1): 99–105.
- Carvalho GA, Nikkhah G, and Samii M. Diagnosis and surgical indications of traumatic brachial plexus lesions from the neurosurgery viewpoint. *Orthopade* 1997; 26(7): 599–605.
- Hems TEJ, Birch R, and Carlstedt T. The role of magnetic resonance imaging in the management of traction injuries to the adult brachial plexus. *J Hand Surg* 1999; 24(5): 550–555.
- Chanlalit C, Vipulakorn K, Jirattanapochai K, et al. Value of clinical findings, electrodiagnosis and magnetic resonance imaging in the diagnosis of root lesions in traumatic brachial plexus injuries. *J Med Assoc Thai* 2005; 88(1): 66–70.
- Zhang L, Xiao T, Yu Q, et al. Clinical value and diagnostic accuracy of 3.0T multi-parameter magnetic resonance imaging in traumatic brachial plexus injury. *Med Sci Monit* 2018; 24: 7199–7205.
- Caranci F, Briganti F, La Porta M, et al. Magnetic resonance imaging in brachial plexus injury. *Musculoskelet Sur* 2013; 97(S2): 181–190.
- van Es HW, Bollen TL, and van Heesewijk HPM. MRI of the brachial plexus: A pictorial review. *Eur J Radiol* 2010; 74(2): 391–402.
- Silbermann-Hoffman O and Teboul F. Post-traumatic brachial plexus MRI in practice. *Diagn Interv Imaging* 2013; 94(10): 925–43.
- Todd M, Shah GV, and Mukherji SK. MR imaging of brachial plexus. *Top Magn Reson Imaging* 2004; 15(2): 113–125.
- Sureka J, Cherian RA, Alexander M, et al. MRI of brachial plexopathies. *Clin Radiol* 2009; 64(2): 208–218.
- Chuang DC. Debates to personal conclusion in peripheral nerve injury and reconstruction: A 30-year experience at Chang Gung Memorial Hospital. *Indian J Plast Surg* 2016; 49(2): 144–150.
- Birch R. Timing of surgical reconstruction for closed traumatic injury to the supraclavicular brachial plexus. *J Hand Surg Eur* 2015; 40(6): 568–572.
- Martin E, Senders JT, DiRisio AC, et al. Timing of surgery in traumatic brachial plexus injury: A systematic review. *J Neurosurg* 2018; 1: 1–13.
- Penkert G, Carvalho G, Nikkhah G, et al. Diagnosis and surgery of brachial plexus injuries. *J Reconstr Microsurg* 1999; 15(1): 3–8.
- Thatte M and Mehta R. Obstetric brachial plexus injury. *Indian J Plast Surg* 2011; 44(3): 380–389.
- Gilbert A, Razaboni R, and Amar-Khodja S. Indications and results of brachial plexus surgery in obstetrical palsy. *Orthop Clin North Am* 1988; 19(1): 91–105.

25. Ochi M, Ikuta Y, Watanabe M, et al. The diagnostic value of MRI in traumatic brachial plexus injury. *J Hand Surg* 1994; 19(1): 55–59.
26. Nakamura T, Yabe Y, Horiuchi Y, et al. Magnetic resonance myelography in brachial plexus injury. *J Bone Joint Surg Br* 1997; 79(5): 764–769.
27. Hayashi N, Masumoto T, Abe O, et al. Accuracy of abnormal paraspinal muscle findings on contrast-enhanced MR images as indirect signs of unilateral cervical root-avulsion injury. *Radiology* 2002; 223(2): 397–402.
28. Wade RG, Takwoingi Y, Wormald JCR, et al. MRI for detecting root avulsions in traumatic adult brachial plexus injuries: A systematic review and meta-analysis of diagnostic accuracy. *Radiology* 2019; 293(1): 125–133.
29. Acharya AM, Cherian BS, and Bhat AK. Diagnostic accuracy of MRI for traumatic adult brachial plexus injury: A comparison study with surgical findings. *J Orthop* 2020; 17: 53–58.
30. Herzberg G, Narakas A, Comtet JJ, et al. Rapports microchirurgicaux des racines du plexus brachial. *Ann Chir Main* 1985; 4(2): 120–133.